Journal of Solid State Chemistry **150,** 121–127 (2000)
doi:10.1006/jssc.1999.8557, available online at http://www.idealibrary.com on IDEAL®

# Structural Transformations in Three-Dimensional Crystalline $GeSe_2$ at High Pressures and High Temperatures

Andrzej Grzechnik,* Svein Stølen,† Egil Bakken,† Tor Grande,‡ and Mohamed Mezouar§

*Max-Planck-Institut für Festkörperforschung, Heisenbergstrasse 1, D-70569 Stuttgart, Germany; †Department of Chemistry, University of Oslo, Postbox 1033, N-0315 Oslo, Norway; ‡Department of Chemistry, Norwegian University of Science and Technology, N-7034 Trondheim, Norway; and §European Synchrotron Radiation Facility, B.P. 220, F-38000 Grenoble, France
E-mail: andrzej@servix.mpi-stuttgart.mpg.de

Received September 8, 1999; in revised form October 20, 1999; accepted October 22, 1999

**Germanium diselenide $GeSe_2$ is studied *in situ* at the pressure range 2–6 GPa using angle-dispersive X-ray diffraction in a large volume Paris–Edinburgh cell. The structure at 2 GPa and 698 K, solved with direct methods in the $I\bar{4}$ space group ($a = 5.5073(3)$ Å, $c = 9.9374(8)$ Å, $Z = 4$), is three dimensional with all the $GeSe_4$ tetrahedra sharing their corners. Anomalous lattice expansion along the *c* axis with increasing pressure and pressure-induced structural variations are explained by anisotropic lattice distortions due to cooperative tiltings of the rigid $GeSe_4$ units.** © 2000 Academic Press

## INTRODUCTION

Amorphous and crystalline phases of silicon and germanium dioxides have been thoroughly studied over several decades because of their importance for understanding both natural and technological systems. The phase diagrams and the kinetics of the phase transitions in $SiO_2$ have been determined with several experimental and theoretical methods (1). On the other hand, the high-pressure behavior of tetrahedral amorphous and crystalline dichalcogenide phases ($MeX_2$; *Me*: Si, Ge; *X*: S, Se) is less known and understood. The long-range ordering of their crystal structures depends on the connectivity of the $MX_4$ tetrahedra. The edge sharing reduces the cross-linking between the tetrahedra, and at ambient pressures $SiS_2$ and $SiSe_2$ have a one-dimentional structure (*Ibam*) with edge-sharing $SiX_4$ units only (2). The connectivity of the $GeX_4$ units in $GeS_2$ and $GeSe_2$ at atmospheric conditions is quite unique, and 50% of the tetrahedra are connected via corners into chains while the other half form $Ge_2X_8$ double units sharing edges. Such a connectivity scheme leads to a layered structure ($P2_1/c$) (3).

As inferred from the quenched products obtained through high-pressure and high-temperature syntheses, there is a tendency for disulfides and dichalcogenides to adopt the three-dimensional ($I\bar{4}2d$) (4–7) or two-dimensional $HgI_2$ ($P4_2/nmc$) (5,6) structure at high pressures. Both types have a common $Me_4X_{10}$ unit consisting of four corner-sharing tetrahedra. Linking this unit could give either the two-dimensional ($P4_2/nmc$) or the three-dimensional ($I\bar{4}2d$) lattice (8). In addition to tetrahedral modifications, an octahedral $CdI_2$-type structure ($P\bar{3}m1$), already taken by $SiTe_2$ at atmospheric pressure (9), was proposed to be stable for $GeS_2$ and $GeSe_2$ above 6 GPa (6). High-pressure experiments carried out *in situ* show that $GeS_2$ and $GeSe_2$ become amorphous above about 7 GPa at room temperature (10). This may indicate that either they fail to transform to a different structure (e.g., the $CdI_2$ structure with sixfold coordinated Me atoms) or that the low-pressure modifications are unstable with regards to their liquid states (1,10). Additionally, a discontinuous *semiconductor-to-metal* transition in glassy $GeSe_2$ is observed in the pressure range where its crystalline counterpart amorphizes (11).

In this study we are interested in *in situ* high-pressure and high-temperature behavior of three-dimensional $GeSe_2$, with all the tetrahedra sharing their corners only. We describe all procedures used to obtain angle-dispersive X-ray diffraction data in a large-volume Paris–Edinburgh cell. Further, we show that the data are suitable for a structural analysis with direct methods, complemented with full Rietveld refinements of the measured patterns. The three-dimensional structure of $GeSe_2$ could serve as a prototype for a tetrahedral framework of the germanium disulfide and diselenide glasses (12). For this reason, the experimental approaches in a large volume Paris–Edinburgh cell presented here could be extended to study high-pressure and high-temperature structural properties of dichalcogenide glasses through computational modeling of disordered networks.

## EXPERIMENTAL

The sample of $GeSe_2$ was prepared by heating stoichiometric amounts of high-purity elements (Goodfellow, UK;



0022-4596/00 $35.00

99.999% Se and 99.999% Ge) at 1173 K for 48 h in an evacuated and sealed silica glass ampoule. The product was ground and annealed at 923 K for 6 weeks to ensure its crystallinity. It was examined by powder X-ray diffraction at room temperature, using a Guinier–Hägg technique ($CrK\alpha_1$ radiation, Si as an internal standard), and was found to have the monoclinic layered structure ($P2_1/c$) (3). No impurities could be detected with X-ray diffraction or with scanning electron and optical microscopies.

Angle-dispersive X-ray diffraction experiments were carried out on the ID30 beamline at the European Synchrotron Radiation Facility. Wavelength selection (0.20215 and 0.26473 Å) and removal of higher-order harmonics were done using a bent Si mirror and Si (1 1 1) monochromator. The beam was collimated to $50 \times 50\ \mu m^2$ by two sets of tungsten carbide slits. Pressures up to 6 GPa and temperatures up to 1123 K were generated using a large-volume Paris–Edinburgh press adapted for X-ray diffraction (13). Samples of powdered $GeSe_2$, 2 mm in height and 0.5 mm in diameter, were put into hexagonal boron nitride (h-BN) cylinders serving as pressure calibrants and located inside high-resistivity graphite furnaces. Such sample assemblies were embedded in "X-ray transparent" boron-epoxy gaskets, compressed between two tungsten carbide anvils. Temperatures were read with thermocouples located in a contact with the samples. The entire setup of the cell was interfaced with an image plate detector for rapid collection of *in situ* X-ray powder diffraction data (14). For each pressure–temperature data point, three images were taken: (a) a first one with the beam passing through the sample, h-BN, and graphite cylinders; (b) a second one with the beam passing through the h-BN and graphite cylinders but not the sample; (c) a third one with the beam passing through the graphite cylinder only. Each two-dimensional image was corrected for spatial distortions and converted to an intensity vs $2\theta$ diffractogram (a resolution of $0.01^\circ$) using the Fit2D software package (15). Subsequently, the same software was used to subtract diffractograms (a) and (b) and diffractograms (b) and (c) in order to minimize the impurity effects in the patterns of the sample and h-BN, respectively. The resulting sample patterns were a subject of further structural analysis, while from the latter ones the h-BN unit cell volumes were extracted to determine the pressures inside the sample assemblies (16). The precision of the temperature and pressure measurements was $\pm 2$ K and $\pm 0.1$ GPa (relative to the h-BN calibration in Ref. (16)), respectively.

## RESULTS AND DISCUSSION

When layered $GeSe_2$ ($P2_1/c$) is compressed to above 2 GPa at temperatures higher than 650 K, there occurs a new phase whose X-ray patterns are similar to the ones of the $I\bar{4}2d$ polymorphs in $GeS_2$ and $GeSe_2$ quenched to atmospheric conditions from high-pressure and high-temperature syntheses (4–7). A close inspection of the X-ray data reveals that the diffractograms collected at the temperature range 600–700 K at pressures 2–6 GPa have admixtures of both phases (Fig. 1), indicating a presence of kinetic effects associated with this transformation. The melting temperature of this new phase is pressure dependent and occurs at 950, 1053, and 1089 K at pressures of 2, 4, and 6 GPa, respectively.

The X-ray pattern collected *in situ* at 2 GPa and 698 K (Fig. 1) can be indexed (17) on an $I$ centered tetragonal cell ($hkl$, $h + k + l = 2n$) with the unit cell dimensions $a = 5.5073(3)$ Å and $c = 9.9374(8)$ Å. However, the systematic extinction condition $00l$, $l = 2n$ violates the symmetry of the $I\bar{4}2d$ space group ($l = 4n$) (18). Based on symmetry arguments, the space group $I\bar{4}$ ($Z = 4$) was chosen for further consideration, as it is a maximal nonisomorphic subgroup of the $I\bar{4}2d$ space group (18). The structure solution was carried out with direct methods for powder diffraction data (19). A full profile fitting and peak decomposition were

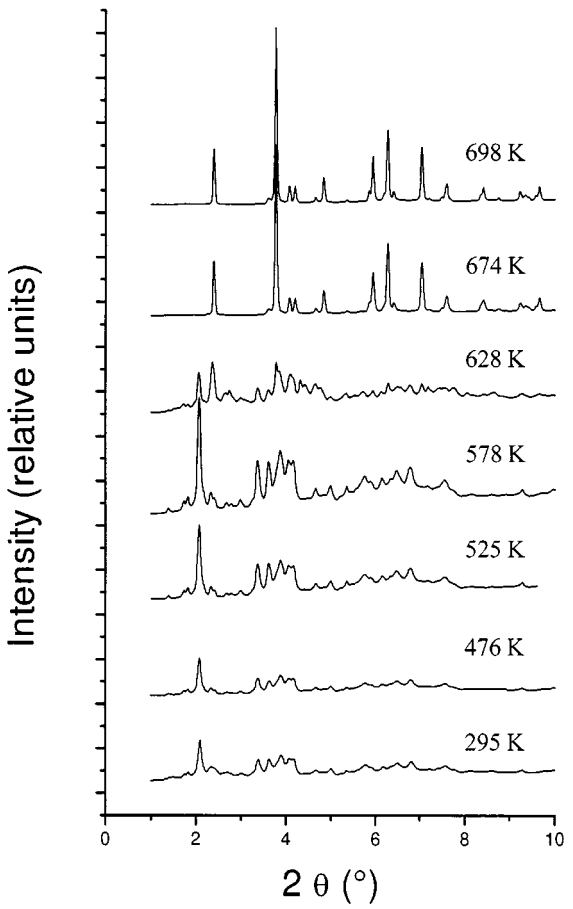


**FIG. 1.** Selected X-ray patterns of $GeSe_2$ as a function of temperature at 2 GPa ($\lambda = 0.20215$ Å).

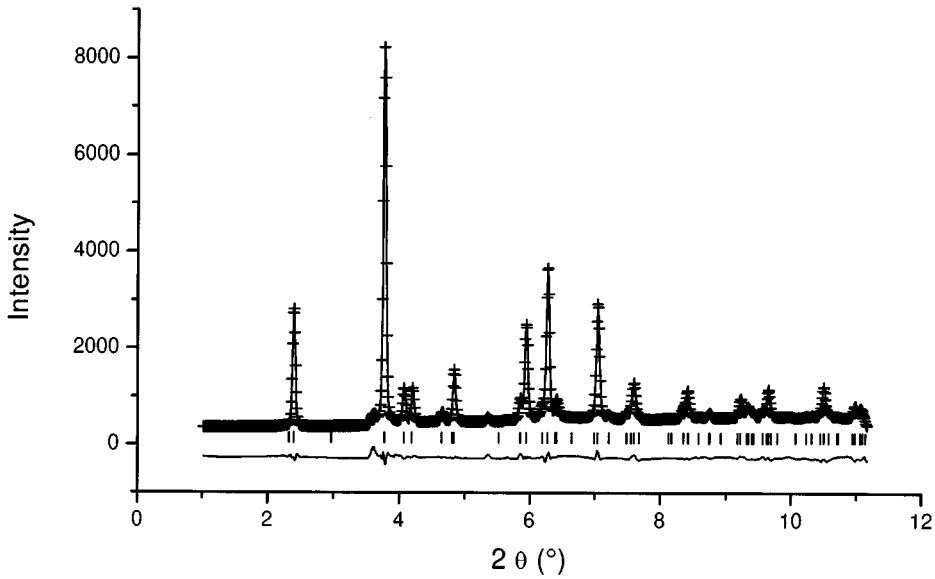


**FIG. 2.** Observed, calculated, and difference XRD profiles for $GeSe_2$ ($I\bar{4}$, $Z = 4$) at 2 GPa and 698 K. Vertical markers indicate Bragg reflections ($\lambda = 0.20215$ Å).

performed with a Le Bail method to extract the structure factor moduli $|F|^2$. A final solution was obtained from a Fourier least-squares procedure. The estimated $R(F^2)$ discrepancy factor between the observed and calculated structure factor moduli (without final Rietveld refinements) was 14.4%. The structure is comprised of two symmetry nonequivalent sets of corner-connected $GeSe_4$ tetrahedra (Fig. 2) with the Ge atoms at the 2*a* (0.5, 0.5, 0.0) and 2*c* (0.5, 0.0, 0.25) special positions and the Se atoms placed at the 8*g* general position (0.752, 0.252, 0.126). The details of a Rietveld refinement (20) and final crystal data are given in Fig. 3 and Tables 1 and 2. In addition to the atomic fractional coordinates and isotropic thermal parameters, the following parameters were allowed to vary during the refinement: 10 background variables of the Chebyshev polynomial, GW and GY variables of the default profile function for constant wavelength diffraction, two cell parameters, a zero point, an overall scale factor—a total of 16 histogram variables.

The $I\bar{4}$ variant is a slight distortion of the $I\bar{4}2d$ one, originating from small displacements of the Se atoms at their sites in the *y* and *z* directions. In the ideal $I\bar{4}2d$ case, the *y* and *z* atomic coordinates for the symmetry-equivalent Se atoms are fixed at 0.25 and 0.125 (the 8*d* Wyckoff site), respectively. Any displacement, however minute, of the atoms lead to lowered symmetry of the lattice (e.g., a superstructure with $Z \geq 4$) and nonequivalency of the Ge and/or Se atoms. The Se atom displacements in the *y* and *z* directions, as determined with direct methods in the $I\bar{4}$ space group, are indeed small, $\Delta y = 0.002$ and $\Delta z = 0.001$ in relative atomic fractional coordinates. The full Rietveld refinement of such a starting model does not change the overall topology, and the respective coordinates do not converge to 0.25 and 0.125. In fact, the relative displacements increase to about $\Delta y = 0.01$ and $\Delta z = 0.003$ (Table 2), resulting in an angular deformation of the $Ge_4Se_{10}$ unit consisting of four corner-sharing tetrahedra (8). The structure solution for the $I\bar{4}2d$ space group was verified for the pattern collected at 2 GPa and 698 K with direct methods, as reported above. The final $R(F^2)$ factor for the lattice with the nondistorted $Ge_4Se_{10}$ unit and the Ge and Se atoms at the 4*a* (0.5, 0.0, 0.25) and 8*d* (0.759, 0.25, 0.125) sites, respectively, was 17.3% (no Rietveld refinement), i.e., higher than the one for the $I\bar{4}$ space group. It should be added that similar considerations are already reported for the case of PON phosphorus oxynitride, for which either $I\bar{4}$ ($Z = 4$) (21) or $P\bar{4}$ ($Z = 4$) (22) structures are discussed as occuring through distortions of the $I\bar{4}2d$ ($Z = 4$) aristotype found in $SiO_2$ crystobalite.

Figure 4 shows the pressure dependence of the lattice parameters at a constant temperature of 741 K. It is striking that the lattice anomalously expands along the *c* axis up to about 5 GPa. At higher pressures, the compressibility along the *c* direction changes, suggesting a structural transformation as discussed below. The Birch–Murnaghan equation of state, with the first pressure derivative of the bulk modulus fixed to 4.0 ($K_0' = 4.0$), was used for fitting the pressure dependence of the unit cell volume between 2 and 4.5 GPa ($T = 741$ K). The extracted unit cell volume ($V_0$) and isothermal bulk modulus ($K_0$), both at zero pressure, are 315.7 (0.8) $Å^3$ and 46.56 (1.84) GPa, respectively. Accordingly, the extrapolated density to zero pressure at 741 K is $\rho = 4.85$ g/cm$^3$.

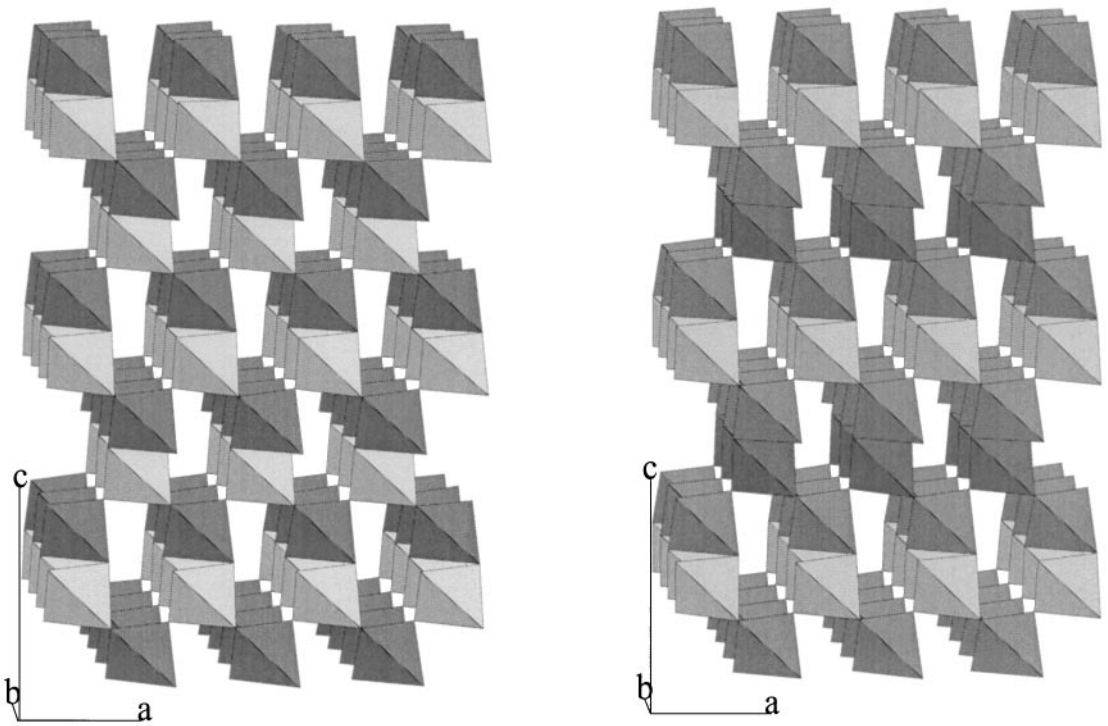


**FIG. 3.** Comparison of the $GeSe_2$ structures in the $I\bar{4}$ (left) and $P\bar{4}$ (right) space groups. Different shading of the tetrahedra indicates symmetry nonequivalent $GeSe_4$ units.

Largely anisotropic compressibilities and an anomalous structure expansion along certain lattice axes are not unusual for low-dimensional solids at high pressures. In the case of three-dimensional compounds, the anisotropic compressibilities could be associated with different degrees of flexibility in their framework built up of rigid polyhedral units. For such solids, compression occurs by coordinated tilting of the polyhedra, rather than by shortening of chemical bonds (23). Figure 5 shows the pressure dependencies of Ge(1)–Se and Ge(2)–Se distances and the Ge(1)–Se–Ge(2) intertetrahedral angle inferred from full Rietveld refinements (the same strategy as before) of the X-ray patterns collected between 2 and 4.5 GPa at constant temperature $T = 741$ K (20). While the bond lengths do not change within the estimated errors, the Ge(1)–Se–Ge(2) angle decreases by about 2° in this pressure range. This observation suggest that the compressibility of three-dimensional $GeSe_2$ is dominated by rotations of rigid tetrahedra. A close examination of this structure (Tables 1 and 2, Fig. 2) shows that the cooperative tiltings associated with diminishing

**TABLE 1**
**Lattice Parameters and Rietveld Refinement Statistics for $GeSe_2$ ($I\bar{4}$, $Z = 4$) at 2 GPa and 698 K**

| | |
|---|---|
| $a$ (Å) | 5.5073(3) |
| $c$ (Å) | 9.9374(8) |
| Volume (Å$^3$) | 301.41(4) |
| Density (g/cm$^3$) | 5.08 |
| $\lambda$ (Å) | 0.20215 |
| $2\theta$ range (°) | 1.01–11.18 |
| Number of observations | 88 |
| $R_{wp}$ | 4.8 |
| $R_p$ | 3.4 |
| $R(F^2)$ | 6.8 |
| $\chi^2$ | 1.56 |

**TABLE 2**
**Rietveld Refined Atomic Coordinates for the Se Atoms, Interatomic Distances (Å), and angles (°) for $GeSe_2$ ($I\bar{4}$, $Z = 4$) at 2 GPa and 698 K**

| | |
|---|---|
| $x$ (Se: 8$g$) | 0.7662(12) |
| $y$ (Se: 8$g$) | 0.260(5) |
| $z$ (Se: 8$g$) | 0.1282(12) |
| Ge(1)–Se | 2.349(18) |
| Se–Ge(1)–Se | 107.1(4) |
| Se–Ge(1)–Se′ | 114.3(8) |
| Ge(2)–Se | 2.380(17) |
| Se–Ge(2)–Se | 104.99(32) |
| Se–Ge(2)–Se′ | 118.9(7) |
| Ge(1)–Se–Ge(2) | 103.28(24) |

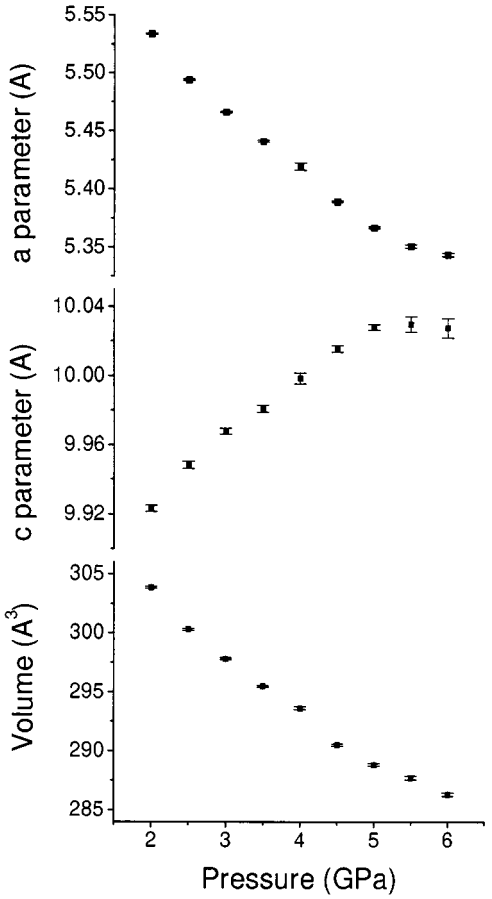


**FIG. 4.** Pressure dependence of lattice parameters in $GeSe_2$ at 741 K.

intertetrahedral angles occur perpendicular to the $c$ axis through an angular deformation of the $Ge_4Se_{10}$ unit consisting of four corner-sharing tetrahedra (8). As a result, the Se–Se distances along the $c$ axis increase, leading to an anomalously stretched lattice in this direction. On the other hand, an enhancement of Se–Se repulsions perpendicular to this axis with increasing pressure could eventually account for the bulk lattice deformation and a transformation of the lattice at about 5 GPa. Our observation of the pressure-induced lattice expansion along the $c$ axis in three-dimensional $GeSe_2$ implies an interesting possibility of a negative thermal expansion in this material. This issue, along with the structure modeling and thermal behavior of $GeSe_2$ liquids generated at high pressures, is a subject of our current research and will be presented later.

The data given in Fig. 4 suggest that the transformation at about 5 GPa occurs without a significant (if any) volume change. Indexing (17) of the pattern at 6 GPa and 773 K (Fig. 6) can be done on a primitive tetragonal lattice, $a = 5.3389(4)$ Å and $c = 10.0361(11)$ Å. An analysis of this pattern and its intensity distribution reveal that the structure is related to the one with $I\bar{4}$ symmetry. From this, we derive the space group $P\bar{4}$ ($Z = 4$) as the one describing the structure of $GeSe_2$ under these conditions, since the $I\bar{4}$ space group is its minimal nonisomorphic supergroup (18). Based on relations for the $I\bar{4}2d$, $I\bar{4}$, and $P\bar{4}$ symmetries, we find three Ge atoms at the special positions 1$a$ (0.0, 0.0, 0.0), 1$d$ (0.5, 0.5, 0.5), and 2$g$ (0.0, 0.5, 0.25) and two sets of nonequivalent Se atoms at the 4$h$ general sites ($x$, $y$, $z$) (Fig. 3). The details of the final Rietveld refinement (20), with the same strategy as before, are shown in Fig. 6 and Tables 3 and 4. As seen in Table 4, the symmetry lowering is mainly due to the Se atom displacements from the ideal positions (in the $I\bar{4}2d$ space group) along the $y$ axis. In the ideal case, each relative difference between the respective $y$ and $z$ atomic coordinates for the two nonequivalent Se atoms should be equal to 0.5. While the $\Delta z$ parameter equal to 0.4993 is close to 0.5 within the estimated standard

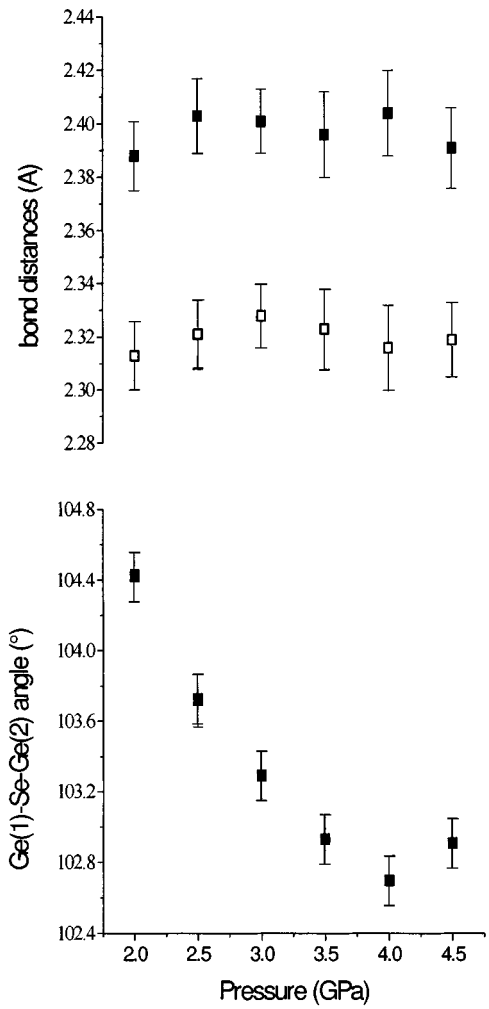


**FIG. 5.** Pressure dependence of interatomic distances and angles for $GeSe_2$ ($I\bar{4}$, $Z = 4$) at 741 K. Open and solid symbols in the plot of distances versus pressure stand for the Ge(1)–Se and Ge(2)–Se bond lengths, respectively.

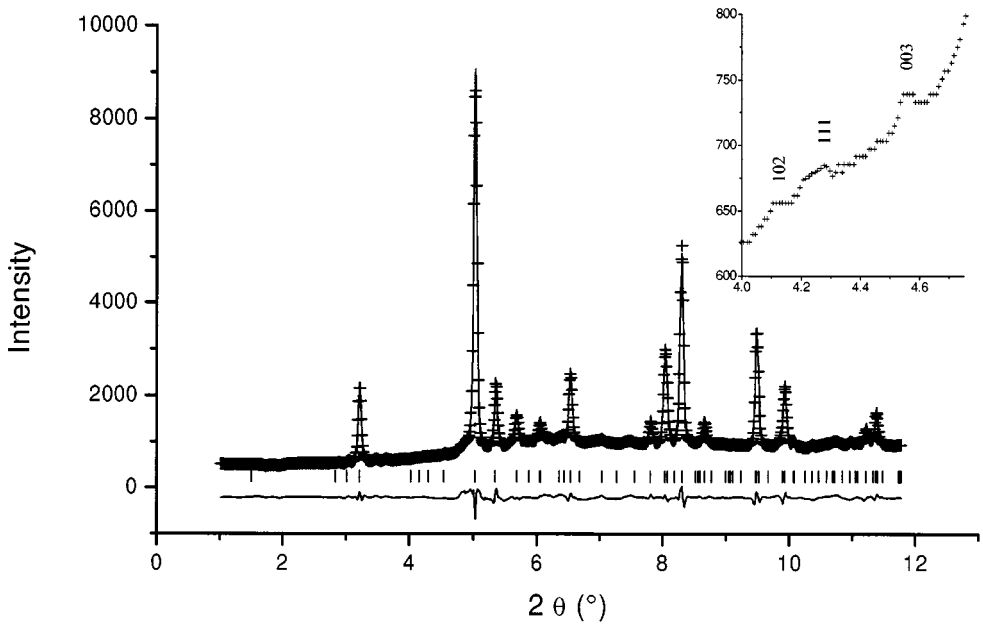


**FIG. 6.** Observed, calculated, and difference XRD profiles for $GeSe_2$ ($P\bar{4}$, $Z = 4$) at 6 GPa and 773 K. Vertical markers indicate Bragg reflections ($\lambda = 0.26473$ Å). In the inset, a part of the pattern is shown with Miller indices for the peaks.

deviations, the $\Delta y = 0.556$ exceeds the combined errors in the atomic coordinate refinements. Unfortunately, our measurements were limited to the pressure range up to 6 GPa, so, based on the present data, it is not possible to infer whether the anomalous expansion of the $I\bar{4}$ lattice, with a subsequent symmetry descent to the $P\bar{4}$ one, can be discussed as a prelude to a phase transition into another denser, possibly sixfold coordinated, phase. One of the examples for such a *four-to-six* transformation in the compounds with $MeX_2$ stoichiometry is the crystobalite → stishovite transition in $SiO_2$ (1). Earlier high-pressure experiments carried out *in situ* show that $GeSe_2$ becomes amorphous above about 7 GPa at room temperature (10). This may indicate either that it fails to transform to a different structure or that the crystalline modification is unstable with regards to its liquid state (1, 10).

The transformation from the two- to the three-dimensional structure in $GeSe_2$ above 2 GPa is sluggish due to

**TABLE 3**
**Lattice Parameters and Rietveld Refinement Statistics for $GeSe_2$ ($P\bar{4}$, $Z = 4$) at 6 GPa and 773 K**

| | |
|---|---|
| $a$ (Å) | 5.3389(4) |
| $c$ (Å) | 10.0361(11) |
| Volume (Å$^3$) | 286.07(4) |
| Density (g/cm$^3$) | 5.35 |
| $\lambda$ (Å) | 0.26473 |
| $2\theta$ range (°) | 1.01–11.78 |
| Number of observations | 85 |
| $R_{wp}$ | 4.4 |
| $R_p$ | 3.3 |
| $R(F^2)$ | 11.1 |
| $\chi^2$ | 2.0 |

**TABLE 4**
**Rietveld Refined Atomic Coordinates for the Se Atoms, Interatomic Distances (Å), and angles (°) for $GeSe_2$ ($P\bar{4}$, $Z = 4$) at 6 GPa and 773 K**

| | | |
|---|---|---|
| $x$ [Se(1): 4$h$] | 0.2739(21) | |
| $y$ [Se(1): 4$h$] | 0.2340(13) | {0.25} |
| $z$ [Se(1): 4$h$] | 0.1280(25) | {0.125} |
| $x$ [Se(2): 4$h$] | 0.7711(20) | |
| $y$ [Se(2): 4$h$] | 0.7700(14) | {0.75} |
| $z$ [Se(2): 4$h$] | 0.6273(32) | {0.625} |
| Ge(1)–Se(1) | 2.31(5) | |
| Ge(3)–Se(1) | 2.38(4) | |
| Ge(2)–Se(2) | 2.41(4) | |
| Ge(2)–Se(3) | 2.26(4) | |
| Se(1)–Ge(1)–Se(1) | 108.0(6) | |
| Se(1)–Ge(1)–Se(1)′ | 112.50(13) | |
| Se(2)–Ge(2)–Se(2) | 106.40(10) | |
| Se(1)–Ge(3)–Se(1) | 118.00(11) | |
| Se(1)–Ge(3)–Se(2) | 103.5(7) | |
| Se(1)–Ge(3)–Se(2)′ | 109.1(9) | |
| Se(2)–Ge(2)–Se(2) | 115.90(21) | |
| Se(2)–Ge(3)–Se(2)′ | 114.10(23) | |
| Ge(1)–Se(1)–Ge(3) | 102.7(4) | |
| Ge(2)–Se(2)–Ge(3) | 103.2(4) | |

*Note.* The numbers in curly brackets are the coordinates derived from the ideal structure in the $I\bar{4}2d$ space group.

kinetic effects associated with breaking of double edge-sharing $Ge_2Se_8$ tetrahedra. Our study shows that the structural variations in three-dimensional $GeSe_2$ studied *in situ* at high pressures and high temperatures can be explained by anisotropic lattice distortions due to the cooperative tiltings of rigid $GeSe_4$ tetrahedra. It is worth noticing that such a three-dimensional structure of $GeSe_2$ (Fig. 3) could serve as one of the prototypes for a tetrahedral framework of the germanium disulfide and diselenide glasses (12). Compression of the glasses at 573 K revealed the presense of two recoverable amorphous compounds for which X-ray diffraction patterns, as measured at atmospheric pressure, were significantly different from the ones for the samples prepared at ambient conditions (5). It is quite likely then that possible structural transitions in the glassy framework of the germanium dichalcogenides (if any) at high pressures and high temperatures, including an anomalous compressibility and thermal expansion, could be similar to the ones in crystalline $GeSe_2$. In analogy to crystalline polymorphism, this behavior in a glass would be called an "amorphous polymorphism" (24). At atmospheric pressure, the two-dimensional polymorph of $GeSe_2$ melts at 1025 K. Our preliminary data on $GeSe_2$ liquids show that the triple point, involving the 2-D and 3-D crystalline phases and the liquid state, is found at about 0.8 GPa and 770 K. Further work is underway to investigate possible "2-D" to "3-D" structural transitions in liquids generated at high pressures, which might lead to the two-liquid behavior of molten $GeSe_2$ in the vicinity of the triple point. As shown here, angle-dispersive X-ray diffraction data taken at high pressure and high temperature utilizing a large-volume Paris–Edinburgh cell and third generation synchrotron radiation can be studied with classical direct methods, complemented with a Rietveld refinement of the measured diffractograms. This encourages efforts to investigate the structure of amorphous compounds under extreme conditions using similar data collection techniques.

## REFERENCES


1. P. J. Heaney, C. T. Prewitt, G. V. Gibbs, Eds., "Silica: Physical Behaviour, Geochemistry and Materials Applications," Reviews in Mineralogy, Vol. 29. Mineralogical Society of America, 1994.
2. J. Peters and B. Krebs, *Acta Crystallogr. B* **24,** 1270 (1982).
3. G. Dittmar and H. Schäfer, *Acta Crystallogr. B* **32,** 2726 (1976); J. Peters and B. Krebs, *Acta Crystallogr. B* **38,** 1270 (1982).
4. C. T. Prewitt and H. S. Young, *Science* **149,** 535 (1965).
5. M. Shimada and F. Dachille, *Inorg. Chem.* **16,** 2094 (1977).
6. Y. Shimizu and T. Kobayashi, *Mem. Inst. Sci. Techn. Meiji Univ.* **21,** 1 (1983)
7. T. Grande, M. Ishii, M. Akaishi, S. Aasland, H. Fjellvåg, S. Stølen, *J. Solid State Chem.* **145,** 167 (1999).
8. A. F. Wells, "Structural Inorganic Chemistry." 5th ed. Clarendon, Oxford, 1984.
9. K. Taketoshi and F. Andoh, *Jpn. J. Appl. Phys.* **34,** 3192 (1995).
10. Z. V. Popovic, M. Holtz, K. Reimann, and K. Syassen, *Phys. Status Solidi* **198,** 533 (1996); Z. V. Popovic, Z. Jaksic, Y. S. Raptis, and E. Anastassakis, *Phys. Rev. B* **57,** 3418 (1998); A. Grzechnik, T. Grande, and S. Stølen, *J. Solid State Chem.* **141,** 248 (1998).
11. M. V. N. Prasad, S. Asokan, G. Parthasarathy, S. S. K. Titus, and E. S. R. Gopal, *Phys. Chem. Glasses* **34,** 199 (1993).
12. K. M. Kandil, M. F. Kotkata, M. L. Theye, A. Gheorghiu, and C. Senemaud, *Phys. Rev. B* **51,** 17565 (1995).
13. P. Grima, A. Polian, M. Gauthier, J. P. Itié, M. Mezouar, G. Weill, and J. M. Besson, *J. Phys. Chem. Solids* **56,** 525 (1995); M. Mezouar, J. M. Besson, G. Syfosse, J. P. Itié, D. Häusermann, and M. Hanfland, *Phys. Status Solidi* **198B,** 403 (1996).
14. M. Thoms, S. Bauchau, M. Kunz, T. Le Bihan, M. Mezouar, D. Häusermann, and D. Strawbridge, *Nucl. Instr. Methods A* **413,** 175 (1998); M. Mezouar, T. Le Bihan, Y. Le Godec, H. Libotte, M. Thoms, and D. Häusermann, *J. Synchrotron Rad.* **6,** 1115 (1999).
15. A. P. Hammersley, S. O. Svensson, M. Hanfland, A. N. Fitch, and D. Häusermann, *High Pressure Res.* **14,** 235 (1996).
16. V. L. Solozhenko and T. Peun, *J. Phys. Chem. Solids* **58,** 1321 (1997).
17. D. Taupin, *J. Appl. Cryst.* **6,** 380 (1973). [As implemented in the CRYSFIRE suite of indexing programs by R. Shirley of Surrey University, UK]
18. "International Tables for Crystallography," Vol. A. Kluwer Academic, Dordrecht, 1983.
19. A. Altomare, M. C. Burla, M. Camalli, B. Carrozzini, G. L. Cascarano, C. Giacovazzo, A. Guagliardi, A. G. G. Moliterni, G. Polidori, and R. Rizzi, *J. Appl. Crystallogr.* **32,** 339 (1999).
20. A. L. Larson and R. B. von Dreele, "Program GSAS: General Structure Analysis System." Los Alamos National Laboratories, Los Alamos, 1994.
21. B.Y. Bondars, A. A. Vitola, T. N. Miller, G. V. Ozolinsh, and Z. Y. Cila, *Latv. PSR Zin. Akad. Vestis Khim. Ser.*, 632 (1977).
22. L. Boukbir, R. Marchand, Y. Laurent, P. Bacher, and G. Roult, *Ann. Chim.* **14,** 475 (1989).
23. J. D. Jorgensen, Z. Hu, S. Teslic, D. N. Argyriou, S. Short, J. S. O. Evans, and A. W. Sleight, *Phys. Rev. B* **59,** 215 (1999).
24. P. Poole, T. Grande, C. A. Angell, and P. F. McMillan, *Science* **149,** 535 (1997).